

Observation of a charged ($D\bar{D}^*$) $^\pm$ mass peak in $e^+e^- \rightarrow \pi D\bar{D}^*$ at $\sqrt{s} = 4.26$ GeV

M. Ablikim¹, M. N. Achasov^{8,a}, O. Albayrak⁴, D. J. Ambrose⁴¹, F. F. An¹, Q. An⁴², J. Z. Bai¹, R. Baldini Ferroli^{19A}, Y. Ban²⁸, J. Becker³, J. V. Bennett¹⁸, M. Bertani^{19A}, J. M. Bian⁴⁰, E. Boger^{21,b}, O. Bondarenko²², I. Boyko²¹, S. Braun³⁷, R. A. Briere⁴, V. Bytev²¹, H. Cai⁴⁶, X. Cai¹, O. Cakir^{36A}, A. Calcaterra^{19A}, G. F. Cao¹, S. A. Cetin^{36B}, J. F. Chang¹, G. Chelkov^{21,b}, G. Chen¹, H. S. Chen¹, J. C. Chen¹, M. L. Chen¹, S. J. Chen²⁶, X. R. Chen²³, Y. B. Chen¹, H. P. Cheng¹⁶, X. K. Chu²⁸, Y. P. Chu¹, D. Cronin-Hennessy⁴⁰, H. L. Dai¹, J. P. Dai¹, D. Dedovich²¹, Z. Y. Deng¹, A. Denig²⁰, I. Denysenko²¹, M. Destefanis^{45A,45C}, W. M. Ding³⁰, Y. Ding²⁴, L. Y. Dong¹, M. Y. Dong¹, S. X. Du⁴⁸, J. Fang¹, S. S. Fang¹, L. Fava^{45B,45C}, C. Q. Feng⁴², P. Friedel³, C. D. Fu¹, J. L. Fu²⁶, O. Fuks^{21,b}, Y. Gao³⁵, C. Geng⁴², K. Goetzen⁹, W. X. Gong¹, W. Gradl²⁰, M. Greco^{45A,45C}, M. H. Gu¹, Y. T. Gu¹¹, Y. H. Guan³⁸, A. Q. Guo²⁷, L. B. Guo²⁵, T. Guo²⁵, Y. P. Guo²⁷, Y. L. Han¹, F. A. Harris³⁹, K. L. He¹, M. He¹, Z. Y. He²⁷, T. Held³, Y. K. Heng¹, Z. L. Hou¹, C. Hu²⁵, H. M. Hu¹, J. F. Hu³⁷, T. Hu¹, G. M. Huang⁵, G. S. Huang⁴², J. S. Huang¹⁴, L. Huang¹, X. T. Huang³⁰, Y. Huang²⁶, T. Hussain⁴⁴, C. S. Ji⁴², Q. Ji¹, Q. P. Ji²⁷, X. B. Ji¹, X. L. Ji¹, L. L. Jiang¹, X. S. Jiang¹, J. B. Jiao³⁰, Z. Jiao¹⁶, D. P. Jin¹, S. Jin¹, F. F. Jing³⁵, N. Kalantar-Nayestanaki²², M. Kavatsyuk²², B. Kloss²⁰, B. Kopf³, M. Kornicer³⁹, W. Kuehn³⁷, W. Lai¹, J. S. Lange³⁷, M. Lara¹⁸, P. Larin¹³, M. Leyhe³, C. H. Li¹, Cheng Li⁴², Cui Li⁴², D. L. Li¹⁷, D. M. Li⁴⁸, F. Li¹, G. Li¹, H. B. Li¹, J. C. Li¹, K. Li¹², Lei Li¹, N. Li¹¹, P. R. Li³⁸, Q. J. Li¹, W. D. Li¹, W. G. Li¹, X. L. Li³⁰, X. N. Li¹, X. Q. Li²⁷, X. R. Li²⁹, Z. B. Li³⁴, H. Liang⁴², Y. F. Liang³², Y. T. Liang³⁷, G. R. Liao³⁵, D. X. Lin¹³, B. J. Liu¹, C. L. Liu⁴, C. X. Liu¹, F. H. Liu³¹, Fang Liu¹, Feng Liu⁵, H. B. Liu¹¹, H. H. Liu¹⁵, H. M. Liu¹, J. P. Liu⁴⁶, K. Liu³⁵, K. Y. Liu²⁴, P. L. Liu³⁰, Q. Liu³⁸, S. B. Liu⁴², X. Liu²³, Y. B. Liu²⁷, Z. A. Liu¹, Zhiqiang Liu¹, Zhiqing Liu¹, H. Loehner²², X. C. Lou^{1,c}, G. R. Lu¹⁴, H. J. Lu¹⁶, J. G. Lu¹, X. R. Lu³⁸, Y. P. Lu¹, C. L. Luo²⁵, M. X. Luo⁴⁷, T. Luo³⁹, X. L. Luo¹, M. Lv¹, F. C. Ma²⁴, H. L. Ma¹, Q. M. Ma¹, S. Ma¹, T. Ma¹, X. Y. Ma¹, F. E. Maas¹³, M. Maggiora^{45A,45C}, Q. A. Malik⁴⁴, Y. J. Mao²⁸, Z. P. Mao¹, J. G. Messchendorp²², J. Min¹, T. J. Min¹, R. E. Mitchell¹⁸, X. H. Mo¹, H. Moeini²², C. Morales Morales¹³, K. Moriya¹⁸, N. Yu. Muchnoi^{8,a}, H. Muramatsu⁴¹, Y. Nefedov²¹, I. B. Nikolaev^{8,a}, Z. Ning¹, S. Nisar⁷, S. L. Olsen²⁹, Q. Ouyang¹, S. Pacetti^{19B}, J. W. Park³⁹, M. Pelizaeus³, H. P. Peng⁴², K. Peters⁹, J. L. Ping²⁵, R. G. Ping¹, R. Poling⁴⁰, E. Prencipe²⁰, M. Qi²⁶, S. Qian¹, C. F. Qiao³⁸, L. Q. Qin³⁰, X. S. Qin¹, Y. Qin²⁸, Z. H. Qin¹, J. F. Qiu¹, K. H. Rashid⁴⁴, C. F. Redmer²⁰, M. Ripka²⁰, G. Rong¹, X. D. Ruan¹¹, A. Sarantsev^{21,d}, S. Schumann²⁰, W. Shan²⁸, M. Shao⁴², C. P. Shen², X. Y. Shen¹, H. Y. Sheng¹, M. R. Shepherd¹⁸, W. M. Song¹, X. Y. Song¹, S. Spataro^{45A,45C}, B. Spruck³⁷, G. X. Sun¹, J. F. Sun¹⁴, S. S. Sun¹, Y. J. Sun⁴², Y. Z. Sun¹, Z. J. Sun¹, Z. T. Sun⁴², C. J. Tang³², X. Tang¹, I. Tapan^{36C}, E. H. Thorndike⁴¹, D. Toth⁴⁰, M. Ullrich³⁷, I. Uman^{36B}, G. S. Varner³⁹, B. Wang¹, D. Wang²⁸, D. Y. Wang²⁸, K. Wang¹, L. L. Wang¹, L. S. Wang¹, M. Wang³⁰, P. Wang¹, P. L. Wang¹, Q. J. Wang¹, S. G. Wang²⁸, X. F. Wang³⁵, X. L. Wang⁴², Y. D. Wang^{19A}, Y. F. Wang¹, Y. Q. Wang²⁰, Z. Wang¹, Z. G. Wang¹, Z. H. Wang⁴², Z. Y. Wang¹, D. H. Wei¹⁰, J. B. Wei²⁸, P. Weidenkaff²⁰, Q. G. Wen⁴², S. P. Wen¹, M. Werner³⁷, U. Wiedner³, L. H. Wu¹, N. Wu¹, S. X. Wu⁴², W. Wu²⁷, Z. Wu¹, L. G. Xia³⁵, Y. X. Xia¹⁷, Z. J. Xiao²⁵, Y. G. Xie¹, Q. L. Xiu¹, G. F. Xu¹, Q. J. Xu¹², Q. N. Xu³⁸, X. P. Xu^{29,33}, Z. Xue¹, L. Yan⁴², W. B. Yan⁴², W. C. Yan⁴², Y. H. Yan¹⁷, H. X. Yang¹, Y. Yang⁵, Y. X. Yang¹⁰, Y. Z. Yang¹¹, H. Ye¹, M. Ye¹, M. H. Ye⁶, B. X. Yu¹, C. X. Yu²⁷, H. W. Yu²⁸, J. S. Yu²³, S. P. Yu³⁰, C. Z. Yuan¹, W. L. Yuan²⁶, Y. Yuan¹, A. A. Zafar⁴⁴, A. Zallo^{19A}, S. L. Zang²⁶, Y. Zeng¹⁷, B. X. Zhang¹, B. Y. Zhang¹, C. Zhang²⁶, C. B. Zhang¹⁷, C. C. Zhang¹, D. H. Zhang¹, H. H. Zhang³⁴, H. Y. Zhang¹, J. L. Zhang¹, J. Q. Zhang¹, J. W. Zhang¹, J. Y. Zhang¹, J. Z. Zhang¹, LiLi Zhang¹⁷, S. H. Zhang¹, X. J. Zhang¹, X. Y. Zhang³⁰, Y. Zhang¹, Y. H. Zhang¹, Z. P. Zhang⁴², Z. Y. Zhang⁴⁶, Zhenghao Zhang⁵, G. Zhao¹, J. W. Zhao¹, Lei Zhao⁴², Ling Zhao¹, M. G. Zhao²⁷, Q. Zhao¹, S. J. Zhao⁴⁸, T. C. Zhao¹, X. H. Zhao²⁶, Y. B. Zhao¹, Z. G. Zhao⁴², A. Zhemchugov^{21,b}, B. Zheng⁴³, J. P. Zheng¹, Y. H. Zheng³⁸, B. Zhong²⁵, L. Zhou¹, X. Zhou⁴⁶, X. K. Zhou³⁸, X. R. Zhou⁴², K. Zhu¹, K. J. Zhu¹, X. L. Zhu³⁵, Y. C. Zhu⁴², Y. S. Zhu¹, Z. A. Zhu¹, J. Zhuang¹, B. S. Zou¹, J. H. Zou¹

(BESIII Collaboration)

¹ Institute of High Energy Physics, Beijing 100049, People's Republic of China

² Beihang University, Beijing 100191, People's Republic of China

³ Bochum Ruhr-University, D-44780 Bochum, Germany

⁴ Carnegie Mellon University, Pittsburgh, Pennsylvania 15213, USA

⁵ Central China Normal University, Wuhan 430079, People's Republic of China

⁶ China Center of Advanced Science and Technology, Beijing 100190, People's Republic of China

⁷ COMSATS Institute of Information Technology, Lahore, Defence Road, Off Raiwind Road, 54000 Lahore

⁸ G.I. Budker Institute of Nuclear Physics SB RAS (BINP), Novosibirsk 630090, Russia

⁹ GSI Helmholtzcentre for Heavy Ion Research GmbH, D-64291 Darmstadt, Germany

¹⁰ Guangxi Normal University, Guilin 541004, People's Republic of China

¹¹ GuangXi University, Nanning 530004, People's Republic of China

¹² Hangzhou Normal University, Hangzhou 310036, People's Republic of China

¹³ Helmholtz Institute Mainz, Johann-Joachim-Becher-Weg 45, D-55099 Mainz, Germany

¹⁴ Henan Normal University, Xinxiang 453007, People's Republic of China

¹⁵ Henan University of Science and Technology, Luoyang 471003, People's Republic of China

¹⁶ Huangshan College, Huangshan 245000, People's Republic of China

¹⁷ Hunan University, Changsha 410082, People's Republic of China

- ¹⁸ Indiana University, Bloomington, Indiana 47405, USA
¹⁹ (A)INFN Laboratori Nazionali di Frascati, I-00044, Frascati, Italy; (B)INFN and University of Perugia, I-06100, Perugia, Italy
²⁰ Johannes Gutenberg University of Mainz, Johann-Joachim-Becher-Weg 45, D-55099 Mainz, Germany
²¹ Joint Institute for Nuclear Research, 141980 Dubna, Moscow region, Russia
²² KVI, University of Groningen, NL-9747 AA Groningen, The Netherlands
²³ Lanzhou University, Lanzhou 730000, People's Republic of China
²⁴ Liaoning University, Shenyang 110036, People's Republic of China
²⁵ Nanjing Normal University, Nanjing 210023, People's Republic of China
²⁶ Nanjing University, Nanjing 210093, People's Republic of China
²⁷ Nankai University, Tianjin 300071, People's Republic of China
²⁸ Peking University, Beijing 100871, People's Republic of China
²⁹ Seoul National University, Seoul, 151-747 Korea
³⁰ Shandong University, Jinan 250100, People's Republic of China
³¹ Shanxi University, Taiyuan 030006, People's Republic of China
³² Sichuan University, Chengdu 610064, People's Republic of China
³³ Soochow University, Suzhou 215006, People's Republic of China
³⁴ Sun Yat-Sen University, Guangzhou 510275, People's Republic of China
³⁵ Tsinghua University, Beijing 100084, People's Republic of China
³⁶ (A)Ankara University, Dogol Caddesi, 06100 Tandoğan, Ankara, Turkey; (B)Dogus University, 34722 İstanbul, Turkey;
(C)Uludag University, 16059 Bursa, Turkey
³⁷ Universitaet Giessen, D-35392 Giessen, Germany
³⁸ University of Chinese Academy of Sciences, Beijing 100049, People's Republic of China
³⁹ University of Hawaii, Honolulu, Hawaii 96822, USA
⁴⁰ University of Minnesota, Minneapolis, Minnesota 55455, USA
⁴¹ University of Rochester, Rochester, New York 14627, USA
⁴² University of Science and Technology of China, Hefei 230026, People's Republic of China
⁴³ University of South China, Hengyang 421001, People's Republic of China
⁴⁴ University of the Punjab, Lahore-54590, Pakistan
⁴⁵ (A)University of Turin, I-10125, Turin, Italy; (B)University of Eastern Piedmont, I-15121, Alessandria, Italy; (C)INFN,
I-10125, Turin, Italy
⁴⁶ Wuhan University, Wuhan 430072, People's Republic of China
⁴⁷ Zhejiang University, Hangzhou 310027, People's Republic of China
⁴⁸ Zhengzhou University, Zhengzhou 450001, People's Republic of China
^a Also at the Novosibirsk State University, Novosibirsk, 630090, Russia
^b Also at the Moscow Institute of Physics and Technology, Moscow 141700, Russia
^c Also at University of Texas at Dallas, Richardson, Texas 75083, USA
^d Also at the PNPI, Gatchina 188300, Russia

We report on a study of the process $e^+e^- \rightarrow \pi^\pm(D\bar{D}^*)^\mp$ at $\sqrt{s} = 4.26$ GeV using a 525 pb^{-1} data sample collected with the BESIII detector at the BEPCII storage ring. A distinct charged structure is observed in the $(D\bar{D}^*)^\mp$ invariant mass distribution. When fitted to a mass-dependent-width Breit-Wigner lineshape, the pole mass and width are determined to be $M_{\text{pole}} = (3883.9 \pm 1.5 \pm 4.2) \text{ MeV}/c^2$ and $\Gamma_{\text{pole}} = (24.8 \pm 3.3 \pm 11.0) \text{ MeV}$. The mass and width of the structure, which we refer to as $Z_c(3885)$, are 2σ and 1σ , respectively, below those of the $Z_c(3900) \rightarrow \pi^\pm J/\psi$ peak observed by BESIII and Belle in $\pi^+\pi^-J/\psi$ final states produced at the same center-of-mass energy. The angular distribution of the $\pi Z_c(3885)$ system favors a $J^P = 1^+$ quantum number assignment for the structure and disfavors 1^- or 0^- . The Born cross section times the $D\bar{D}^*$ branching fraction of the $Z_c(3885)$ is measured to be $\sigma(e^+e^- \rightarrow \pi^\pm Z_c(3885)^\mp) \times \mathcal{B}(Z_c(3885)^\mp \rightarrow (D\bar{D}^*)^\mp) = (83.5 \pm 6.6 \pm 22.0) \text{ pb}$. Assuming the $Z_c(3885) \rightarrow D\bar{D}^*$ signal reported here and the $Z_c(3900) \rightarrow \pi J/\psi$ signal are from the same source, the partial width ratio $\frac{\Gamma(Z_c(3885) \rightarrow D\bar{D}^*)}{\Gamma(Z_c(3900) \rightarrow \pi J/\psi)}$ = $6.2 \pm 1.1 \pm 2.7$ is determined.

PACS numbers: 14.40.Rt, 13.25.Gv, 14.40.Pq

The $Y(4260)$ resonance was first seen by BaBar as a peak in the $e^+e^- \rightarrow \pi^+\pi^-J/\psi$ cross section as a function of e^+e^- center-of-mass (CM) energy [1]. It was subsequently confirmed by CLEO [2] and Belle [3]. Its production via the e^+e^- annihilation process requires the quantum numbers of the $Y(4260)$ to be $J^{PC} = 1^{--}$. A peculiar feature is the absence of any apparent corresponding

structure in the cross sections for $e^+e^- \rightarrow D^{(*)}\bar{D}^{(*)}(\pi)$ in the $\sqrt{s} = 4260$ MeV energy region [4]. This implies a lower-limit partial width of $\Gamma(Y(4260) \rightarrow \pi^+\pi^-J/\psi) > 1 \text{ MeV}$ [5] that is one order-of-magnitude larger than measured values for conventional charmonium meson transitions [6], and indicates that the $Y(4260)$ is probably not a conventional quarkonium state.

A similar pattern is seen in the b -quark sector, where anomalously large cross sections for $e^+e^- \rightarrow \pi^+\pi^-\Upsilon(nS)$ ($n = 1, 2, 3$) at energies around $\sqrt{s} = 10.86$ GeV reported by Belle [7] were subsequently found to be associated with the production of charged bottomonium-like resonances, the $Z_b(10610)^+$ and $Z_b(10650)^+$, both with strong decays to $\pi^+\Upsilon(nS)$ and $\pi^+h_b(mP)$ ($m = 1, 2$) [8]. The $Z_b(10610)^+$ mass is just above the $m_B + m_{B^*}$ threshold and it decays copiously to $B\bar{B}^*$, while the $Z_b(10650)^+$ mass is just above the $2m_{B^*}$ threshold and it decays copiously to $B^*\bar{B}^*$ [9]. Their proximity to the BB^* and $B^*\bar{B}^*$ thresholds as well as their decay patterns suggest that these states may be molecule-like meson-meson virtual states [10]; a subject of considerable interest [11].

Recently BESIII reported the observation of a prominent resonance-like charged structure in the $\pi J/\psi$ invariant mass distribution for $e^+e^- \rightarrow \pi^+\pi^-J/\psi$ events collected at $\sqrt{s} = 4.26$ GeV, dubbed the $Z_c(3900)$. A fit to a Breit-Wigner (BW) resonance lineshape yields $M = (3899.0 \pm 3.6 \pm 4.9)$ MeV/c 2 and $\Gamma = (46 \pm 10 \pm 20)$ MeV [12]. (Here, and elsewhere in this report, the first errors are statistical and the second systematic.) This observation was subsequently confirmed by Belle [13]. The $Z_c(3900)$ mass is ~ 20 MeV/c 2 above the $D\bar{D}^*$ mass threshold, which is suggestive of a virtual $D\bar{D}^*$ molecule-like structure [14, 15]; *i.e.*, a charmed-sector analog of the $Z_b(1610)$. (BESIII also reported resonance-like structures in charged $D^*\bar{D}^*$ and πh_c systems at $M \simeq 4025$ MeV, which may be a charmed-sector analog of the $Z_b(10650)$ [16].) Another possibility is a diquark-dantiquark state [17]. It is important to measure the rate for $Z_c(3900)$ decays to $D\bar{D}^*$ and compare it to that of the $\pi J/\psi$.

Here we report the observation of a peak in the $(D\bar{D}^*)^-$ invariant-mass distribution in $e^+e^- \rightarrow \pi^+(D\bar{D}^*)^-$ annihilation events at $\sqrt{s} = 4.26$ GeV with a 525 pb $^{-1}$ data sample detected by the BESIII detector at the BEPCII electron-positron collider. In the following, this structure is referred to as the $Z_c(3885)$. The $\pi^+(D\bar{D}^*)^-$ final states are selected by means of a partial reconstruction technique in which only the bachelor π^+ and one final-state D meson are detected, and the presence of the \bar{D}^* is inferred from energy-momentum conservation. (In this report, the inclusion of charge conjugate states is always implied.) We perform parallel analyses of both isospin channels ($\pi^+D^0D^{*-}$ and $\pi^-D^+\bar{D}^{*0}$) as a consistency check. The D mesons are reconstructed in the $D^0 \rightarrow K^-\pi^+$ and $D^+ \rightarrow K^-\pi^+\pi^+$ decay channels.

The BESIII detector is a large-solid-angle magnetic spectrometer consisting of a 50-layer Helium-gas-based main cylindrical drift chamber (MDC), a barrel-like arrangement of time-of-flight scintillation counters (TOF), and an electromagnetic calorimeter comprised of CsI(Tl) crystals located inside a superconducting solenoid coil that provides a 1 T magnetic field. An iron flux-return located outside of the coil is instrumented with resistive

plate chambers to identify muons. The charged particle momentum resolution for 1 GeV/c charged tracks is 0.5% and the energy resolution for 1 GeV photons is 2.5%. Measurements of dE/dx in the MDC and flight times in the TOF are combined to determine pion, kaon and proton identification (ID) probabilities. The hypothesis with the highest ID probability is assigned to each particle. The detector is described in detail in Ref. [18].

To study the detector response and identify potential backgrounds, we use samples of Monte Carlo (MC) simulated events that are produced by the EVTGEN generator [19] in conjunction with KKMC [20], which generates ISR photons, and simulated using a GEANT4-based [21] software package [22]. In addition to signal channels and various potential background processes, we simulated generic events using Born cross sections for charmonium processes that have been measured, Lundcharm to generate production of other, non-measured charmonium states [23] and PYTHIA for unmeasured hadronic final states [24].

For the π^+D^0 -tag analysis, we select events with three or more well reconstructed charged tracks in the polar angle region $|\cos\theta| < 0.93$, with points of closest approach to the e^+e^- interaction point that are less than 10 cm in the beam direction and 1 cm in the plane perpendicular to the beam direction. At least one of the tracks is required to be negatively charged and identified as a kaon. In addition, we require at least two positively charged tracks that are identified as π^+ mesons. We designate $K^-\pi^+$ combinations with invariant mass within 15 MeV/c 2 of m_{D^0} as D^0 candidates. For events with two or more $K^-\pi^+$ combinations, we retain the one with invariant mass closest to m_{D^0} . For the π^-D^+ -tag analysis, the selection is the same except for the requirement of an additional π^- track that is identified as the bachelor pion and the mass requirement $|M(K^-\pi^+\pi^+) - m_{D^+}| < 15$ MeV/c 2 to select the D^+ candidates.

The left panel of Fig. 1 shows the distribution of masses recoiling against the detected π^+D^0 system [25], where a prominent peak at $m_{D^{*-}}$ is evident. The solid-line histogram shows the same distribution for MC-simulated $e^+e^- \rightarrow \pi^+D^0D^{*-}$, $D^0 \rightarrow K^-\pi^+$ three-body phase-space events. Because of the limited phase space, some events from the isospin partner decay $\pi^+Z_c(3885)^-$, $Z_c(3885)^- \rightarrow D^-D^{*0}$, where the detected D^0 is a decay product of the D^{*0} , also peak near $m_{D^{*-}}$, as shown by the dashed histogram that is for MC-simulated $e^+e^- \rightarrow \pi^+Z_c(3885)^-$, $Z_c(3885)^- \rightarrow D^-D^{*0}$, $D^{*0} \rightarrow \gamma$ or π^0D^0 decays. Here the mass and width of the $Z_c(3885)$ are set to our final measured values. Since the $D\bar{D}^*$ invariant mass distribution is equivalent to the bachelor pion recoil mass spectrum, the shape of the $Z_c(3885) \rightarrow D\bar{D}^*$ signal peak is not sensitive to the parentage of the D meson that is used for the event tagging. The right panel of Fig. 1 shows the corresponding plots for the π^-D^+ tagged events, where the solid histogram shows the contribu-

tion from MC-simulated $e^+e^- \rightarrow \pi^- D^+ \bar{D}^{*0}$ three-body phase-space events. Here, also, the $\pi^- D^+$ -tagged event sample that is used to study $\pi^- D^+ \bar{D}^{*0}$ includes some cross feed from the $\pi^- Z_c(3885)^+, Z_c(3885)^+ \rightarrow \bar{D}^0 D^{*+}$ signal channel, where the D^+ used for tagging is a decay product of the D^{*+} . The dashed histogram is from MC-simulated $e^+e^- \rightarrow \pi^- Z_c(3885)^+, Z_c(3885)^+ \rightarrow \bar{D}^0 D^{*+}, D^{*+} \rightarrow \pi^0 D^+$ events.

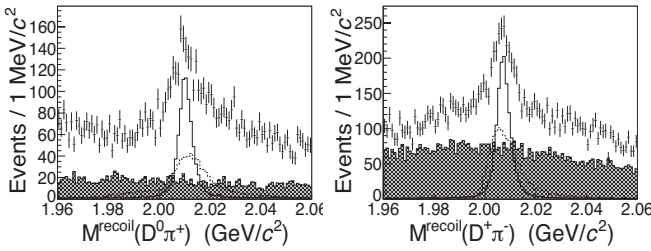


FIG. 1. The πD recoil mass distribution for the $\pi^+ D^0$ - (left) and $\pi^- D^+$ -tagged (right) events. Points with errors are data, the hatched histogram shows the events from the D mass sidebands. The solid and dashed histograms are described in the text.

We apply a two-constraint kinematic fit to the selected events, where we constrain the invariant mass of the D^0 (D^+) candidate tracks to be equal to m_{D^0} (m_{D^+}) and the mass recoiling from the $\pi^+ D^0$ ($\pi^- D^+$) to be equal to $m_{D^{*-}}$ ($m_{\bar{D}^{*0}}$). If there is more than one bachelor pion candidate in an event, we retain the one with the smallest χ^2 from the kinematic fit. Events with $\chi^2 < 30$ are selected for further analysis. For the $\pi^+ D^0$ -tag analysis, we require $M(\pi^+ D^0) > 2.02$ GeV to reject the events of the type $e^+e^- \rightarrow D^{*+} D^{*-}, D^{*+} \rightarrow \pi^+ D^0$. The left (right) panel of Fig. 2 shows the distribution of $D^0 D^{*-}$ ($D^+ \bar{D}^{*0}$) invariant masses recoiling from the bachelor pion for the $\pi^+ D^0$ ($\pi^- D^+$) tagged events. The two distributions are similar and both have a distinct peak near the $m_D + m_{\bar{D}^*}$ mass threshold. For cross-feed events, the reconstructed D meson is not in fact recoiling from a \bar{D}^* and the efficiency for satisfying these selection requirements decreases with increasing $D\bar{D}^*$ mass. Studies with phase-space MC event samples show that this acceptance variation is not sufficient to produce a peaking structure.

To characterize the observed enhancement and determine the signal yield, we fit the histograms in the left and right panels of Fig. 2 using a mass-dependent-width Breit-Wigner (BW) lineshape to model the signal and smooth threshold functions to represent the non-peaking background. For the signal, we use $dN/dm_{D\bar{D}^*} \propto (k^*)^{2\ell+1} |BW_{Z_c}(m_{D\bar{D}^*})|^2$, where k^* is the Z_c momentum in the e^+e^- rest frame, ℓ is the $\pi-Z_c$ relative orbital angular momentum and $BW_{Z_c}(m_{D\bar{D}^*}) \propto \frac{\sqrt{m_{D\bar{D}^*}\Gamma_{Z_c}}}{m_{Z_c}^2 - m_{D\bar{D}^*}^2 - im_{Z_c}\Gamma_{Z_c}}$. Here $\Gamma_{Z_c} = \Gamma_0(q^*/q_0)^{2L+1}(m_{Z_c}/m_{D\bar{D}^*})$, where $q^*(m_{D\bar{D}^*})$ is the D momentum in the $Z_c(3885)$ rest frame, $q_0 = q^*(m_{Z_c})$

and L is the $D-\bar{D}^*$ orbital angular momentum. In the default fits, we set $\ell = 0$, $L = 0$ and leave m_{Z_c} and Γ_0 as free parameters. We multiply the BW by a polynomial determined from a fit to the MC-determined mass-dependent efficiency to form the signal probability density function (PDF). Mass resolution effects are less than 1 MeV/ c^2 and, thus, ignored. For the non-peaking background for the $M(D\bar{D}^*)$ distribution, we use: $f_{bkg}(m_{D\bar{D}^*}) \propto (m_{D\bar{D}^*} - M_{\min})^c(M_{\max} - m_{D\bar{D}^*})^d$, where M_{\min} and M_{\max} are the minimum and maximum kinematically allowed masses, respectively. The exponents c and d are free parameters determined from the fits to the data.

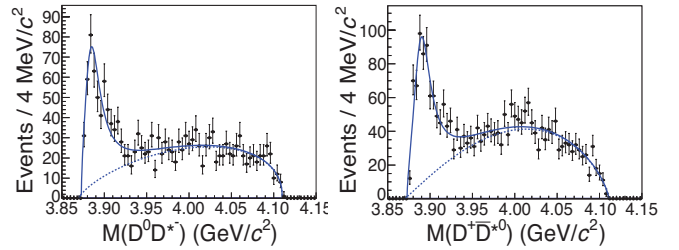


FIG. 2. The $M(D^0 D^{*-})$ (left) and $M(D^+ \bar{D}^{*0})$ (right) distributions for selected events. The curves are described in the text.

The results of the fits are shown as solid curves in Fig. 2. The dashed curves show the fitted non-resonant background. The fitted BW masses and widths from the $\pi^+ D^0$ ($\pi^- D^+$) tagged sample are 3889.2 ± 1.8 MeV/ c^2 and 28.1 ± 4.1 MeV (3891.8 ± 1.8 MeV/ c^2 and 27.8 ± 3.9 MeV), where the errors are statistical only. Since the mass and width of a mass-dependent-width BW are model dependent and may differ from the actual resonance properties [27], we solve for $P = M_{\text{pole}} - i\Gamma_{\text{pole}}/2$, the position in the complex (M, Γ) plane where the BW denominator is zero, and use M_{pole} and Γ_{pole} to characterize the mass and width of the $Z_c(3885)$ peak. Table I lists the pole masses and widths for the $\pi^+ D^0$ and $\pi^- D^+$ tagged samples.

TABLE I. The pole mass M_{pole} and width Γ_{pole} , signal yields and fit quality (χ^2/ndf) for the two tag samples.

Tag	$M_{\text{pole}}(\text{MeV}/c^2)$	$\Gamma_{\text{pole}}(\text{MeV})$	Z_c signal (evts)	χ^2/ndf
$\pi^+ D^0$	3882.3 ± 1.5	24.6 ± 3.3	502 ± 41	54/54
$\pi^- D^+$	3885.5 ± 1.5	24.9 ± 3.2	710 ± 54	60/54

Monte Carlo studies of possible sources of peaking backgrounds in the $D\bar{D}^*$ mass distribution show that processes of the type $e^+e^- \rightarrow D\bar{D}_X, \bar{D}_X \rightarrow \bar{D}^*\pi$, would produce a near-threshold reflection peak in the $D\bar{D}^*$ mass distribution, where D_X denotes a $D^*\pi$ resonance with mass near the upper kinematic boundary. This boundary, $\sqrt{s} - m_D$, is 30 MeV/ c^2 below the mass of the lightest established $D^*\pi$ resonance, the $D_1(2420)$,

with $M_{D_1} = 2421.3 \pm 0.6$ MeV/c² and $\Gamma_{D_1} = 27.1 \pm 2.7$ MeV [6], which suggests that contributions from $D\bar{D}_1(2420)$ final states, either from $Y(4260) \rightarrow D\bar{D}_1$ decays or non-resonant $e^+e^- \rightarrow D\bar{D}_1$ production, are beyond the kinematic reach at $\sqrt{s} = 4260$ MeV and, therefore, are small. However, some models for the $Y(4260)$ attribute it to a bound $D\bar{D}_1$ molecular state [14], where sub-threshold $\bar{D}_1 \rightarrow \bar{D}^*\pi$ decays might be important and, possibly, produce a reflection peak in the $D\bar{D}^*$ mass distribution that mimics a $Z_c(3885)$ signal.

To study this possibility, we separated the events into two samples according to $|\cos \theta_{\pi D}| > 0.5$ and $|\cos \theta_{\pi D}| < 0.5$, where $\theta_{\pi D}$ is the angle between the bachelor pion and the D meson directions in the $Z_c(3885)$ rest frame. The $D\bar{D}_1$ MC events predominantly have $|\cos \theta_{\pi D}| > 0.5$ while, in contrast, $e^+e^- \rightarrow \pi Z_c$ signal-MC sample has similar numbers of events with $|\cos \theta_{\pi D}| > 0.5$ and $|\cos \theta_{\pi D}| < 0.5$. We define an asymmetry parameter $\mathcal{A} = (n_{>0.5} - n_{<0.5})/(n_{>0.5} + n_{<0.5})$, where $n_{>0.5}$ ($n_{<0.5}$) is the fitted number of $Z_c(3885)$ signal events for $|\cos \theta_{\pi D}| > 0.5$ (< 0.5). For the data, $\mathcal{A}_{\text{data}} = 0.12 \pm 0.06$, close to the MC value for $e^+e^- \rightarrow \pi Z_c(3885)$: $\mathcal{A}_{\text{MC}}^{\pi Z_c} = 0.02 \pm 0.02$, and far from the MC result for the $e^+e^- \rightarrow D\bar{D}_1$ hypothesis: $\mathcal{A}_{\text{MC}}^{D\bar{D}_1} = 0.43 \pm 0.04$. We conclude that the $D\bar{D}_1$ contribution to our observed $Z_c(3885) \rightarrow D\bar{D}^*$ signal is small.

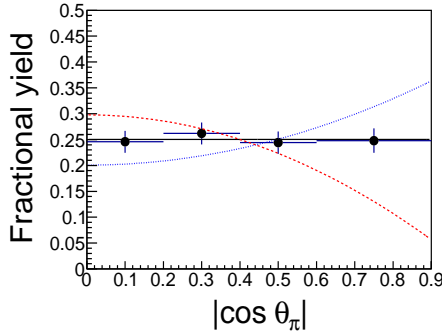


FIG. 3. $(1/N_{\text{tot}})dN/d|\cos \theta_\pi|$ versus $|\cos \theta_\pi|$ for $Z_c(3885)$ events in data. The solid, dashed and dotted curves show expectations for $J^P = 1^+$, 0^- and 1^- , respectively.

If the J^P quantum numbers of the $Z_c(3885)$ are 1^+ , the relative π - Z_c orbital in the decay $Y(4260) \rightarrow \pi Z_c$ can be S - and/or D -waves. Since the decay is near threshold, the D -wave contribution should be small, in which case the $dN/d|\cos \theta_\pi|$ distribution would be flat, where θ_π is the bachelor pion's polar angle relative to the beam direction in the CM. If $J^P = 0^-$, the decay can only proceed via a P -wave and is polarized with $J_z = \pm 1$; in this case $dN/d\cos \theta_\pi \propto \sin^2 \theta_\pi$. Similarly, $J^P = 1^-$ also implies a P -wave with an expected distribution that goes as $1 + \cos^2 \theta$. Parity conservation excludes $J^P = 0^+$.

We sliced the data into four $|\cos \theta_\pi|$ bins and repeated the fits described above for each bin. The $|\cos \theta_\pi|$ -dependence of the efficiency is determined from sig-

nal MC event samples. Figure 3 shows the efficiency-corrected fractional signal yield *vs.* $|\cos \theta_\pi|$. The solid (dashed) curve shows the result of a fit to a flat ($\sin^2 \theta_\pi$) distribution. The data agree well with the flat expectation for $J^P = 1^+$, with $\chi^2/\text{ndf} = 0.44/3$ and disagree with those for $J^P = 0^-$, for which $\chi^2/\text{ndf} = 32/3$, and 1^- , where $\chi^2/\text{ndf} = 16/3$.

We use the fitted numbers of signal events for the π^+D^0 -tagged sample, $N_{\pi^+}(Z_c^- \rightarrow (D\bar{D}^*)^-)$, and for the π^-D^+ -tagged sample, $N_{\pi^-}(Z_c^+ \rightarrow (D\bar{D}^*)^+)$ to make two independent measurements of the product of the cross section and branching fraction $\sigma(e^+e^- \rightarrow \pi Z_c) \times \mathcal{B}(Z_c \rightarrow D\bar{D}^*)$. We assume isospin symmetry and, for the π^+D^0 -tagged channel, use the relation

$$\begin{aligned} & \sigma(e^+e^- \rightarrow \pi^+ Z_c(3885)^-) \times \mathcal{B}(Z_c^- \rightarrow (D\bar{D}^*)^-) \quad (1) \\ &= \frac{N_{\pi^+}^{-}(Z_c^- \rightarrow (D\bar{D}^*)^-)}{\mathcal{L}(1+\delta)\mathcal{B}_{D^0 \rightarrow K^- \pi^+}(\epsilon_1^0 + \epsilon_2^0)/2}, \end{aligned}$$

where $\mathcal{L} = 525 \pm 5$ pb⁻¹ is the integrated luminosity, $(1+\delta) = 0.87 \pm 0.04$ is the radiative correction factor [28], $\epsilon_1^0 = 0.46$ is the efficiency for $\pi^+ Z_c^-$, $Z_c^- \rightarrow D^0 D^*$ -MC events and $\epsilon_2^0 = 0.21$ is the efficiency for $\pi^+ Z_c^-$, $Z_c^- \rightarrow D^- D^{*0}$, $D^{*0} \rightarrow \gamma/\pi^0 D^0$ MC events. The resulting value is $\sigma(e^+e^- \rightarrow \pi^+ Z_c^-) \times \mathcal{B}(Z_c(3885)^- \rightarrow (D\bar{D}^*)^-) = 84.6 \pm 6.9$ pb, where the error is statistical only.

For the π^-D^+ -tagged channel, we use

$$\begin{aligned} & \sigma(e^+e^- \rightarrow \pi^- Z_c(3885)^+) \times \mathcal{B}(Z_c^+ \rightarrow (D\bar{D}^*)^+) \quad (2) \\ &= \frac{N_{\pi^-}(Z_c^+ \rightarrow (D\bar{D}^*)^+)}{\mathcal{L}(1+\delta)\mathcal{B}_{D^+ \rightarrow K^- \pi^+}(\epsilon_1^+ + \epsilon_2^+ \mathcal{B}_{D^{*+} \rightarrow \pi^0 D^+})/2}, \end{aligned}$$

where $\epsilon_1^+ = 0.34$ is the efficiency for $\pi^- Z_c^+$, $Z_c^+ \rightarrow D^+ \bar{D}^{*0}$ MC events and $\epsilon_2^+ = 0.24$ is the efficiency for $\pi^- Z_c^+$, $Z_c^+ \rightarrow \bar{D}^0 D^{*+}$, $D^{*+} \rightarrow \pi^0 D^+$ MC events. The result is $\sigma(e^+e^- \rightarrow \pi^- Z_c(3885)^+) \times \mathcal{B}(Z_c^+ \rightarrow (D\bar{D}^*)^+) = 82.3 \pm 6.3$ pb (statistical error only) and in good agreement with that for the π^+D^0 -tag sample, which justifies our assumption of isospin invariance.

Systematic errors include uncertainties from tracking, particle ID, D mass and decay branching fraction, kinematic fit, signal and background shapes, MC efficiency, $Y(4260)$ lineshape, the radiative correction factor and the luminosity. The uncertainties from tracking and particle ID are both 1% per track. The uncertainties from D selection and the kinematic fit are determined from a $e^+e^- \rightarrow D^{*+} D^{*-}$ control sample that has the same final state as the $\pi^+D^0 D^{*-}$ signal events. The variation of the efficiency over the $Z_c(3885)$ mass uncertainty range is included as a systematic error. The systematic errors for the luminosity and $Y(4260)$ resonance parameters are taken from Ref. [12]. For the signal shape error we use the difference between the pole mass & width and signal yield from the fits that use a mass-dependent width (default) and the mass, width and yield from fits with

TABLE II. Contributions to systematic errors on the pole mass, pole width and signal yield. When two values are listed, the first is for $\pi^+ D^0$ tags and the second for $\pi^- D^+$ tags.

Source	$M_{\text{pole}}(\text{MeV}/c^2)$	$\Gamma_{\text{pole}}(\text{MeV})$	$\sigma \times \mathcal{B} (\%)$
Tracking & PID			$\pm 4/6$
D mass req.			± 1
D^0/D^+ Bfs.			± 1
Kinematic fit			± 4
Signal BW shape	$\pm 1/2$	± 3	± 5
Bkgd shape	$\pm 4.0/3.8$	$\pm 10.4/10.7$	± 24
MC efficiency			$\pm 6/3$
$Y(4260)$ lineshape			± 0.6
Luminosity			± 1
Rad. corr.			± 5
Sum in quadrature	$\pm 4.1/4.3$	$\pm 10.8/11.1$	$\pm 26.4/26.3$

mass-independent-width BW lineshapes. The most significant contributions to the systematic errors are related to the choice of background shape. For this, we compare results from the default fit with those that use a symmetric exponential threshold function and the distribution of wrong-sign πD events extracted from the data.

In all the fits used in this analysis, it is assumed that the $\pi Z_c(3885)$ system is produced in an S -wave and the $D\bar{D}^*$ system produced in the decay of the $Z_c(3885)$ is also in an S -wave. Attempts to fit the peak using P -wave line shapes all failed to converge. This compatibility with S -wave is consistent with the observed $\cos \theta_\pi$ distribution.

The contributions from each source are summarized in Table II. We assume that the errors from the different sources are uncorrelated and use the sums in quadrature as the total systematic errors.

For the final mass, width and cross section values, we use weighted averages of the results from the two tag modes, with the near-complete correlations between the systematic errors taken into account. The results are listed in Table III, where we also include results for the $Z_c(3900) \rightarrow \pi J/\psi$ taken from Ref. [12] for comparison. When statistical and systematic errors are added in quadrature, the $Z_c(3885)$ mass is about 2σ lower than that for the $Z_c(3900)$ and the width is 1σ lower.

TABLE III. Parameters for the $Z_c(3885) \rightarrow D\bar{D}^*$ reported here and those for the $Z_c(3900) \rightarrow \pi J/\psi$ taken from Ref. [12].

	$Z_c(3885) \rightarrow D\bar{D}^*$	$Z_c(3900) \rightarrow \pi J/\psi$
Mass (MeV/ c^2)	$3883.9 \pm 1.5 \pm 4.2$	$3899 \pm 3.6 \pm 4.9$
Γ (MeV)	$24.8 \pm 3.3 \pm 11.0$	$46 \pm 10 \pm 20$
$\sigma \times \mathcal{B}$ (pb)	$83.5 \pm 6.6 \pm 22.0$	$13.5 \pm 2.1 \pm 4.8$

In summary, we report observation of a strong, near-threshold enhancement, $Z_c(3885)$, in the $D\bar{D}^*$ invariant mass distribution in the process $e^+e^- \rightarrow \pi^\pm(D\bar{D}^*)^\mp$ at

$\sqrt{s} = 4.26$ GeV. Attempts to fit the $Z_c(3885)$ peak with a P -wave BW lineshape failed to converge, and the $|\cos \theta_\pi|$ distribution agrees well with S -wave expectations; both results favor a $J^P = 1^+$ quantum number assignment. Other $J \leq 1$ assignments are eliminated.

An important question is whether or not the source of the $Z_c(3885) \rightarrow D\bar{D}^*$ structure is the same as that for the $Z_c(3900) \rightarrow \pi J/\psi$. The fitted $Z_c(3885)$ mass is about 2σ below that of the $Z_c(3900)$ [12, 13]. However neither fit considers the possibility of interference with a coherent non-resonant background that could shift the results. A J^P quantum number determination of the $Z_c(3900)^\pm$ would provide an additional test of this possibility.

Assuming the $Z_c(3885)$ structure reported here is due to the $Z_c(3900)$, the ratio of partial decay widths is determined to be $\frac{\Gamma(Z_c(3885) \rightarrow D\bar{D}^*)}{\Gamma(Z_c(3900) \rightarrow \pi J/\psi)} = 6.2 \pm 1.1 \pm 2.7$ (here the main systematic errors are almost entirely uncorrelated). This ratio is much smaller than typical values for decays of conventional charmonium states above the open charm threshold. For example: $\Gamma(\psi(3770) \rightarrow D\bar{D})/\Gamma(\psi(3770) \rightarrow \pi^+\pi^-J/\psi) = 482 \pm 84$ [6] and $\Gamma(\psi(4040) \rightarrow D^{(*)}\bar{D}^{(*)})/\Gamma(\psi(4040) \rightarrow \eta J/\psi) = 192 \pm 27$ [26]. This suggests the influence of very different dynamics in the $Y(4260)$ - $Z_c(3900)$ system.

The BESIII collaboration thanks the staff of BEPCII and the computing center for their strong support. This work is supported in part by the Ministry of Science and Technology of China Contract No. 2009CB825200; National Natural Science Foundation of China (NSFC) Contract Nos. 10821063, 10825524, 10835001, 10935007, 11125525, 11235011; Joint Funds of the National Natural Science Foundation of China under Contract Nos. 11079008, 11179007, 11079027; Chinese Academy of Sciences (CAS) Large-Scale Scientific Facility Program; CAS Contract Nos. KJCX2-YW-N29, KJCX2-YW-N45; 100 Talents Program of CAS; German Research Foundation (DFG) Contract No. Collaborative Research Center CRC-1044; Istituto Nazionale di Fisica Nucleare, Italy; Ministry of Development of Turkey Contract No. DPT2006K-120470; U. S. Department of Energy Contract Nos. DE-FG02-04ER41291, DE-FG02-05ER41374, DE-FG02-94ER40823; U.S. National Science Foundation; University of Groningen (RUG); Helmholtzzentrum für Schwerionenforschung GmbH (GSI) Darmstadt; Korean National Research Foundation (NRF) Grant No. 20110029457.

-
- [1] B. Aubert *et al.* (BaBar Collaboration), Phys. Rev. Lett. **95**, 142001 (2005).
 - [2] Q. He *et al.* (CLEO Collaboration), Phys. Rev. D **74**, 091104(R) (2006).
 - [3] C.Z. Yuan *et al.* (Belle Collaboration), Phys. Rev. Lett. **99**, 182004 (2005).
 - [4] G. Pakhlova *et al.* (Belle Collaboration), Phys. Rev. Lett.

- 98**, 092001 (2007); Phys. Rev. Lett. **100**, 062001 (2008); Phys. Rev. D **77**, 011103 (2008); Phys. Rev. Lett. **101**, 172001 (2008); and Phys. Rev. D **80**, 091101 (2009).
- [5] X.H. Mo *et al.*, Phys. Lett. **B640**, 182 (2006).
- [6] J. Beringer *et al.* (Particle Data Group), Phys. Rev. D **86**, 010001 (2012).
- [7] K.-F. Chen *et al.* (Belle Collaboration), Phys. Rev. Lett. **100**, 112001 (2008).
- [8] A. Bondar *et al.* (Belle Collaboration), Phys. Rev. Lett. **108**, 122001 (2012).
- [9] I. Adachi *et al.* (Belle Collaboration), arXiv:1209.6450v2 [hep-exp].
- [10] A.E. Bondar *et al.*, Phys. Rev. D **84**, 054010 (2011), D.V. Bugg, Europhys. Lett. **96**, 11002 (2011), I.V. Danilkin, V.D. Orlovsky and Yu.A. Simonov, Phys. Rev. D **85**, 034012 (2012), C.-Y. Cui, Y.-L. Liu and M.-Q. Huang, Phys. Rev. D **85**, 054014 (2012), T. Guo, L. Cao, M.-Z. Zhou and H. Chen, arXiv:1106.2284 [hep-ph], and J.-R. Zhang, M. Zhong and M.-Q. Huang Phys. Lett. **B704**, 312 (2011).
- [11] See, for example, M.B. Voloshin and L.B. Okun, JETP Lett. **23**, 333 (1976); M. Bander, G.L. Shaw and P. Thomas, Phys. Rev. Lett. **36**, 695 (1977); A. De Rujula, H. Georgi and S.L. Glashow, Phys. Rev. Lett. **38**, 317 (1977); A.V. Manohar and M.B. Wise, Nucl. Phys. B **339**, 17 (1993); N.A. Törnqvist, hep-ph/0308277 (2003); F.E. Close and P.R. Page, Phys. Lett. B **578**, 119 (2003); C.-Y. Wong, Phys. Rev. C **69**, 055202 (2004); S. Pakvasa and M. Suzuki, Phys. Lett. B **579**, 67 (2004); E. Braaten and M. Kusunoki, Phys. Rev. D **69**, 114012 (2004); E.S. Swanson, Phys. Lett. B **588**, 189 (2004); D. Gammelmann and E. Oset, Phys. Rev. D **80**, 014003 (2009) & Phys. Rev. D **81**, 014029 (2010).
- [12] M. Ablikim *et al.* (BESIII Collaboration), Phys. Rev. Lett. **110**, 252001 (2013).
- [13] Z.Q. Liu *et al.* (Belle Collaboration), Phys. Rev. Lett. **110**, 252002 (2013).
- [14] Q. Wang, C. Hanhart and Q. Zhao, Phys. Rev. Lett. **111**, 132003 (2013).
- [15] N. Mahajan, arXiv:1304.1301 [hep-ph], M.B. Voloshin, Phys. Rev. D **87**, 091501 (2013), J.-R. Zhang, Phys. Rev. D **87**, 116004 (2013), F.-K. Guo, *et al.*, Phys. Rev. D **88**, 054007 (2013) and C.-Y. Cui *et al.*, arXiv:1304.1850.
- [16] M. Ablikim *et al.* (BESIII Collaboration), arXiv:1308.2760 [hep-ex] and M. Ablikim *et al.* (BESIII Collaboration), arXiv:1309.1896 [hep-ex].
- [17] R. Faccini *et al.*, Phys. Rev. D **87**, 111102R (2013); and M. Karliner and S. Nussinov, JHEP **1307**, 153 (2013). See, also, A. Ali, C. Hambrock and W. Wang, Phys. Rev. D **85**, 054011 (2012).
- [18] M. Ablikim *et al.* (BESIII Collaboration), Nucl. Instrum. and Methods Phys. Res., Sect. A **614**, 345 (2010).
- [19] D.J. Lange, Nucl. Instrum. and Methods Phys. Res., Sect. A **462**, 152 (2001).
- [20] S. Jadach, B.F.L. Ward, and Z. Was, Comput. Phys. Commun. **130**, 260 (2000); Phys. Rev. D **63**, 113009 (2001).
- [21] S. Agostinelli *et al.* (Geant4 Collaboration), Nucl. Instrum. and Methods Phys. Res., Sect. A **506**, 250 (2003).
- [22] Z.Y. Deng, *et al.*, High Energy Phys. Nucl. Phys. **30** 371, (2006).
- [23] R.G. Ping *et al.*, Chinese Phys. C **32**, 599 (2008).
- [24] T. Sjöstrand, S. Mrenna and P. Skands, JHEP **026**, 0605 (2006).
- [25] We minimize the effect of the D mass resolution by plotting $M^{\text{recoil}} = RM(\pi D) + M(D) - m_D$, where $RM(\pi D)$ is the recoil mass inferred from four-momentum conservation and $M(D)$ is the measured D mass.
- [26] M. Ablikim *et al.* (BESIII Collaboration), Phys. Rev. D **86**, 071101 (2012).
- [27] See, for example, A.R. Bohm and N.L. Harshman, arXiv:hep-ph/0001206 and references cited therein.
- [28] We use a second-order QED calculation and unpublished BESIII energy-dependent measurements of $\sigma(e^+e^- \rightarrow \pi DD^*)$ to compute the radiative correction; see E. A. Kuraev and V. S. Fadin, Yad. Fiz. **41**, 733 (1985) [Sov. J. Nucl. Phys. **41**, 466 (1985)].